A global water vapor data set obtained by merging the SSMI and MODIS data

Bo-Cai Gao,[1] Pui K. Chan,[2,3] and Rong-Rong Li[3,4]

Received 2 June 2004; revised 27 July 2004; accepted 19 August 2004; published 18 September 2004.

[1] At present, the column amount of atmospheric water vapor over clear land surfaces and over oceanic areas with sun glint is operationally retrieved from radiances measured with near-IR channels of the Moderate Resolution Imaging SpectroRadiometer (MODIS) instruments on board the NASA Terra and Aqua Spacecraft platforms. TPW over oceans has also been derived operationally from radiances measured by the Special Sensor Microwave Imagers (SSMI) on board different spacecraft. We report in this letter that a global water vapor data product with improved quality can be obtained by merging the monthly-mean MODIS near-IR TPW data over land and the SSMI TPW data over water surfaces. Major characteristics of the seasonal variations of TPW are described. Examples of water vapor anomalies associated with the 2002 El Niño event are presented. We expect that the merged TPW data product will have useful applications for the study of the global hydrological cycle. *INDEX TERMS:* 1610 Global Change: Atmosphere (0315, 0325); 1640 Global Change: Remote sensing; 1655 Global Change: Water cycles (1836); 1694 Global Change: Instruments and techniques; 3360 Meteorology and Atmospheric Dynamics: Remote sensing. **Citation:** Gao, B.-C., P. K. Chan, and R.-R. Li (2004), A global water vapor data set obtained by merging the SSMI and MODIS data, *Geophys. Res. Lett.*, *31*, L18103, doi:10.1029/2004GL020656.

1. Introduction

[2] Hydrological processes play an important role in weather and climate by determining the energetics and dynamics. Yet many aspects of the hydrological processes are not well understood and there are still large uncertainties in various hydrologic parameters, particularly over data sparse areas such as the oceans and remote land areas [*Webster*, 1994]. Total precipitable water (TPW) is the amount of liquid water that would result if all the water vapor in the atmospheric column of unit area were condensed. TPW distribution contains valuable information on the vigor of the hydrological processes and moisture transport in the atmosphere. Accurate global measurement, modeling and long-term prediction of water vapor is the primary goal of the Global Water Vapor Project which is a component of GEWEX (Global Energy and Water Cycle Experiment) [*World Climate Research Program* (*WCRP*), 1997]. Long-term global measurement of TPW will be useful in studying the global hydrological cycle, documenting seasonal and inter-annual variations, and verifying model output.

[3] Global measurement of TPW is made possible by satellite observations. Measurement of TPW can be obtained based on atmospheric water vapor absorption or emission of radiation, either at the near-infrared or microwave wavelengths. Using microwave techniques, TPW can be retrieved under both cloudy and clear sky conditions. With the near-infrared techniques, TPW can be retrieved only under clear sky condition. Nevertheless, microwave retrieval cannot be made over land because of the large uncertainties in microwave emissivities of land surfaces. On the other hand, near-infrared retrieval can be made both over land and oceanic areas with sunglint [*Gao and Kaufman*, 2003]. Therefore, it is a good idea to combine the near-infrared retrieval over land and the microwave retrieval over ocean to form a new global data set. Here the Terra MODIS data over land and the SSMI data over ocean are merged to form a global TPW data set.

2. Methods

2.1. MODIS Near-IR Water Vapor Retrieval

[4] The MODIS instrument [*Salomonson et al.*, 1989; *King et al.*, 2003] has 36 channels covering the spectral region between 0.4 and 15 μm. Five narrow channels centered near 0.865, 0.905, 0.935, 0.94, and 1.24 μm are useful for remote sensing of water vapor. An operational algorithm for retrieving column water vapor amounts from these near-IR channels was previously developed [*Gao and Kaufman*, 2003]. The algorithm relies on observations of water vapor attenuation of near-IR solar radiation reflected by surfaces. The algorithm computes the ratios of apparent reflectance at channels in the 0.94-μm water vapor absorption band and the atmospheric window channels at 0.865 μm and 1.24 μm. The ratios largely remove the effects of the variation of surface reflectance with wavelength for most land surfaces and these ratios represent the atmospheric transmittances. The column water vapor amounts are derived from the transmittances using a table searching procedure. The lookup tables were generated with a line-by-line code and the HITRAN2000 line database [*Rothman et al.*, 1998]. Typical errors in the derived water vapor values are estimated to be in the range between 5% and 10%.

[5] The MODIS data are commonly processed into different levels from Level 1 (radiances or brightness temperatures that have been geolocated), to Level 2 (derived geophysical data products at the same resolution and location as the Level 1 data), to Level 3 (variables mapped

[1]Remote Sensing Division, Naval Research Laboratory, Washington, D. C., USA.
[2]Science Systems and Applications, Inc., Lanham, Maryland, USA.
[3]Also at NASA Goddard Space Flight Center, Greenbelt, Maryland, USA.
[4]University of Maryland at Baltimore County, Baltimore, Maryland, USA.

Copyright 2004 by the American Geophysical Union.
0094-8276/04/2004GL020656$05.00

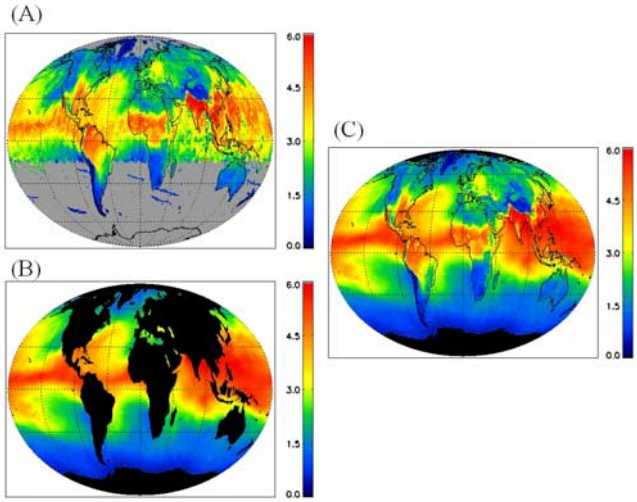

Figure 1. The monthly mean total precipitable water distribution for July 2001 obtained (a) from MODIS near-IR retrieval, (b) from SSMI, and (c) by merging the MODIS image over land areas and the SSMI image over water areas.

onto uniform space-time grid scale) [*King et al.*, 2003]. The MODIS atmospheric data products are now available for public access. The Level 2 water vapor products are generated at the 1-km spatial resolution. Through integration of the Level 2 products, the Level 3 daily, 8-day, and monthly-mean water vapor products are generated globally at a 1° by 1° latitude-longitude grid resolution. Figure 1a shows a monthly-mean MODIS near-IR water vapor image for July 2001. A number of water vapor distribution patterns over land surfaces are observed. For example, very small amounts of water vapor are observed over southern Australia, the Tibetan Plateau in Asia, and Andes Mountains in South America. The Indian Continent and Indo-China regions are very humid. The near-IR water vapor products are not generated over major portions of oceanic areas (masked as gray areas in this plot) in the southern hemisphere due to the lack of reflective ocean surface (sun glint) for this austral winter month.

2.2. SSMI Water Vapor Retrieval

[6] Over water surfaces, TPW was previously retrieved from passive microwave radiometer measurements with the Nimbus series of experimental instruments [*Prabhakara et al.*, 1982]. There are several algorithms for the retrieval of oceanic TPW using measurements near the center of a weak water vapor absorption line at 22 GHz [e.g., *Ferraro et al.*, 1996; *Alishouse et al.*, 1990; *Wentz*, 1997]. Currently there are at least three Special Sensor Microwave Imagers (SSMI) or similar sensors on board different spacecraft for operational retrieval of TPW over oceans using the algorithm developed by *Wentz and Spencer* [1998]. In this algorithm, the near-surface wind speed, TPW, and columnar cloud liquid water are retrieved simultaneously by matching the measured brightness temperatures at 19.35, 22.235, 37, and 85.5 GHz with theoretically simulated brightness temperatures. Figure 1b shows a monthly-mean SSMI water vapor image for July 2001. The image was processed from data downloaded from the web site of Remote Sensing Systems, Inc. (http://www.ssmi.com/). Very smooth water vapor distributions over oceanic areas are observed. TPW is not retrieved at the microwave frequencies over land because of the large microwave emissivities of land surfaces (∼0.95) in comparison to the small emissivities of water surfaces (∼0.5) [*Ferraro et al.*, 1996]. As a result, the land areas are masked in black in this figure.

2.3. Merging of Terra MODIS and SSMI Monthly-Mean Water Vapor Data

[7] MODIS provides water vapor retrievals over land while SSMI does not. SSMI provides water vapor retrievals over most water surfaces, including oceans and major lakes. MODIS does not provide retrievals over large oceanic areas where sun glint is absent. Although MODIS provides the retrievals over oceanic areas with sun glint, the spatial distributions of TPW are not nearly as smooth and contiguous as those in the SSMI image. This is because the frequency of occurrence of sun glint conditions for the MODIS measurements is far less than the frequency of SSMI measurements and MODIS retrievals occur under clear sky condition only. In view of these limitations, it is advantageous to merge the MODIS data over land and SSMI data over water to form a new water vapor data set. Figure 1c shows a merged water vapor image for July 2001.

3. Results and Applications

[8] By combining the Terra MODIS near-IR TPW data over land surfaces and the SSMI data over water surfaces, we have obtained a merged TPW data set that extends from March 2000 to present. Two applications of the data set, one for the study of seasonal variations of water vapor and the other for the study of El Niño-related anomalies, are described below.

[9] The merged data set can be used to study the seasonal variations of water vapor distributions on the global scale. Figures 2a, 2b, 2c, and 2d show the monthly-mean water vapor image for January, April, July, and October 2002, respectively. A prominent feature is the seasonal migration of the belt of maximum TPW, which is in accord with the

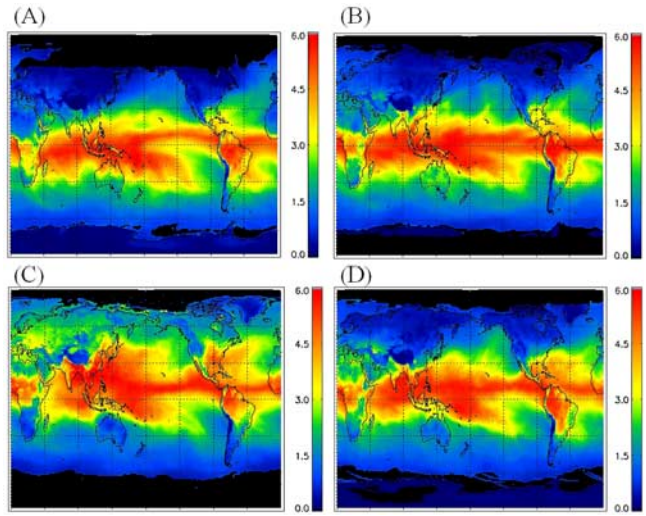

Figure 2. Total precipitable water distribution for (a) January, (b) April, (c) July and (d) October 2002 from MODIS and SSMI.

seasonal migration of the intertropical convergence zone and the onset and withdrawal of monsoons. From January to July the belt of maximum TPW, particularly over the western Pacific, expand and move northward, stretching over to the summer monsoon region of India and China and to the southeastern part of the United States. From October to January as the cold continental anticyclones gradually establish, bringing cold dry air to southern United States and southern Asia, the belt shrinks and moves towards the southern hemisphere. In order to reveal the relationship between TPW and sea surface temperatures (SSTs), we show in Figure 3 the monthly-mean SST image for October 2002, which is obtained from the National Center for Environmental Prediction (NCEP). The spatial patterns of TPWs in Figure 2d resemble the SST patterns in Figure 3. The maximum TPW is located within the region of high SST (28C contour) in the West Pacific. The dry tongue in the East Pacific (see Figure 2d) almost coincides with the cold tongue (see Figure 3). This resemblance is expected because the capacity of the atmosphere to retain water vapor depends strongly on the temperature [*Peixoto and Oort*, 1992].

[10] The merged data set can also be used to study the anomalies in water vapor distributions associated with the 2002 El Niño event. Figure 4a shows a water vapor difference image (1/2002–1/2001) over Australia and western Pacific. In January 2002, the southeastern part of Australia was very dry, and major fire events occurred. The difference image shows that TPW in southeastern Australia for January 2002 are about 1 cm less than those over the same areas for January 2001. A narrow elongated area east to Papua New Guinea appears "red" in this image, which indicates that the area has more water vapor in January 2002 than in January 2001. This observed feature is due to the eastward movement of the "warmpool" during the El Niño year. Figure 4b shows a SST difference image (1/2002–1/2001) covering the same areas as those in Figure 4a. The image was processed from the SST data downloaded from the web site of Remote Sensing Systems, Inc. The SST data were derived from measurements acquired with the TRMM (Tropical Rainfall Measuring Mission) Microwave Imager (TMI) [*Wentz et al.*, 2000]. A narrow elongated "red" area east of Indonesia is also seen in this image. This feature confirms the eastward movement of the "warmpool" during the 2002 El Niño year. By comparing the Figure 4b image with the Figure 4a image over water surfaces, it is seen that the areas with increased SST values in January 2002 generally correspond to areas with increased TPW values.

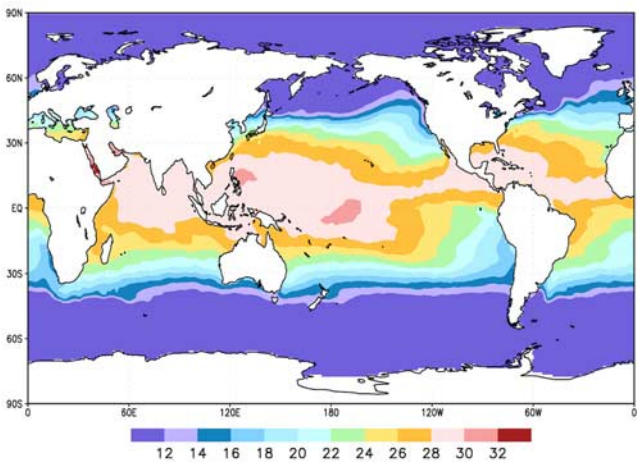

Figure 3. NCEP sea surface temperature distribution for October 2002.

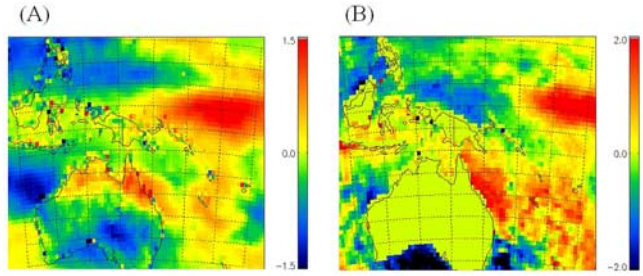

Figure 4. (a) A water vapor difference image (1/2002–1/2001) over Australia and western Pacific, and (b) a sea surface temperature (SST) difference image for the same months and over the same area as (a). The color bar in (a) ranges for water vapor differences from −1.5 cm (blue) to +1.5 cm (red). The color bar in (b) ranges for SST differences of −2 K (blue) to +2 K (red).

4. Discussions

[11] We have provided two examples of applications of the merged Terra MODIS and SSMI TPW data set in Section 3. The data set should have many other practical applications, for example, the study of transport of water vapor from the Gulf of Mexico to the eastern and central U.S. during the spring and summer months.

[12] The Aqua Spacecraft is equipped with both MODIS instrument and microwave instrument named AMSR-E (Advanced Microwave Scanning Radiometer for EOS). Two monthly-mean water vapor products are now produced separately from measurements taken from the Aqua Spacecraft. The NASA Aqua Project will not produce the merged water vapor product (MODIS over land and AMSR-E over water), similar to the one illustrated in Figure 1c. It is very difficult to produce such a merged product using data acquired with different instruments in the Aqua operational computing environment. In order to produce a merged water vapor data set from Aqua measurements, one can order the L3 monthly-mean Aqua MODIS and AMSR-E water vapor data sets from NASA Distributed Active Archive Centers, and then conduct his/her own data merging.

5. Summary

[13] A global TPW data set is obtained by merging the results from MODIS near infrared and SSMI microwave retrievals. The merged data set covers the period from March 2000 to present. The data set can be used for the study of seasonal and annual variations of water vapor on regional and global scales. We expect that the data set will have useful applications in the study of global hydrological cycles.

[14] **Acknowledgment.** This research was supported by the NASA Office of Earth Science and by the U.S. Office of Naval Research.

References

Alishouse, J., A. A. Snyder, J. Vongsathorn, and R. R. Ferraro (1990), Determination of oceanic total precipitable water from the SSM/I, *IEEE Trans. Geosci. Remote Sensing*, *28*, 811–816.

Ferraro, R. R., F. Z. Weng, N. C. Grody, and A. Basist (1996), An eight-year (1987–1994) time series of rainfall, clouds, water vapor, snow cover, and sea ice derived from SSM/I measurements, *Bull. Am. Meteorol. Soc.*, *77*, 891–905.

Gao, B.-C., and Y. J. Kaufman (2003), Water vapor retrievals using Moderate Resolution Imaging Spectrometer (MODIS) near-IR channels, *J. Geophys. Res.*, *108*(D13), 4389, doi:10.1029/2002JD003023.

King, M. D., W. P. Menzel, Y. J. Kaufman, D. Tanre, B.-C. Gao, S. Platnick, S. A. Ackerman, L. A. Remer, R. Pincus, and P. A. Hubanks (2003), Cloud and aerosol properties, precipitable water, and profiles of temperature and humidity from MODIS, *IEEE Trans. Geosci. Remote Sens.*, *41*, 442–458.

Peixoto, J. P., and A. H. Oort (1992), *Physics of Climate*, 520 pp., Am. Inst. of Phys., College Park, Md.

Prabhakara, C., H. D. Chang, and A. T. C. Chang (1982), Remote sensing of precipitable water over the oceans from Nimbus 7 microwave measurements, *J. Appl. Meteorol.*, *31*, 5968.

Rothman, L. S., et al. (1998), The HITRAN molecular spectroscopic database and HAWKS (HITRAN Atmospheric Workstation): 1996 edition, *J. Quant. Spectrosc. Radiat. Transfer*, *60*, 665–710.

Salomonson, V. V., W. L. Barnes, P. W. Maymon, H. E. Montgomery, and H. Ostrow (1989), MODIS: Advanced facility instrument for studies of the Earth as a system, *IEEE Trans. Geosci. Remote Sens.*, *27*, 145–153.

Webster, P. J. (1994), The role of hydrological processes in ocean-atmosphere interactions, *Rev. Geophys.*, *32*, 427–476.

Wentz, F. J. (1997), A well-calibrated ocean algorithm for special sensor microwave/imager, *J. Geophys. Res.*, *102*, 8703–8718.

Wentz, F. J., and R. W. Spencer (1998), SSM/I rain retrievals within a unified all-weather ocean algorithm, *J. Atmos. Sci.*, *55*, 1613–1627.

Wentz, F. J., C. Gentemann, D. Smith, and D. Chelton (2000), Satellite measurements of sea surface temperature through clouds, *Science*, *288*, 847–850.

World Climate Research Program (WCRP) (1997), Report of the first workshop of the WCRP/GEWEX Water Vapour Project (GVaP), informal report, Geneva, Switzerland.

B.-C. Gao, Remote Sensing Division, Code 7232, Naval Research Laboratory, 4555 Overlook Ave., SW, Washington, DC 20375, USA. (gao@nrl.navy.mil)

P. K. Chan and R.-R. Li, Climate and Radiation Branch, NASA Goddard Space Flight Center, Greenbelt, MD 20771, USA.